



Research Article

© 2024 Lopez Ramos et al.

This is an open access article licensed under the Creative Commons Attribution-NonCommercial 4.0 International License (<https://creativecommons.org/licenses/by-nc/4.0/>)

Received: 12 January 2024 / Accepted: 19 February 2024 / Published: 5 March 2024

High Stress Economic Scenario on Renewable Energy Integration with Genetic-Firework Hybrid Algorithm

Nicolas Lopez Ramos¹

Altin Hoti¹

Takeaki Toma¹

¹College of Engineering and Technology,
American University of the Middle East,
Kuwait

DOI: <https://doi.org/10.36941/ajis-2024-0051>

Abstract

This work models a hard economic scenario in which inflation rate is set to 7%, the price of diesel is increasing, the price of electricity purchased from the power grid is inflated and there is a top limit for daily purchasable electricity on a region, in which there is an attempt to introduce renewable energy on a private property of the size of a residential house of 5 people. The optimal microgrid configuration is approximated by the new Hybrid Genetic-Fireworks Algorithm working in conjunction with a Monte Carlo simulation to find the annual worth, and comparing results with a Genetic Algorithm and a Fireworks Algorithm. The components considered are: solar panels, wind turbines, diesel generators, electric batteries, converters, and a connection to the power grid. The objective is to maximize annual worth. The results show that a cost of energy (COE) of 2.0603 USD per kWh is achievable in such scenario, and recommends the further use of the Hybrid Genetic-Fireworks Algorithm for this type or Renewable Energy Integration studies, as it outperformed their 2 counterparts in this work.

Keywords: Hybrid Genetic-Firework Algorithm, Genetic Algorithm, Fireworks Algorithm, Monte Carlo Simulation, Renewable Energy Integration, Hybrid Microgrid

1. Introduction

Electricity is a resource that is vastly used nowadays on an extensive array of applications ranging from healthcare, industrial processes, private residential purposes, and several others word wide. Access to electricity has reached a status of being considered an almost basic need due to its importance for daily operations of many processes: and as such, one can conclude that the continuity in the availability of this resource is of upmost importance for future generations. Moreover, the utilization of electricity has been steadily increasing for the last 50 years (IEA, 2021), and there is no clear reason to believe that this world trend will change soon. Additionally, an argument could be made that the demand level of electricity is directly correlated to population level itself, as it is apparent that more people will likely consume more electricity. If this argument is true, we can support the basis that electricity demand will likely continue to rise, as it is projected that world

population will also continue to increase in the following years (UN, 2022) from 8 billion to approximately 10 billion people in the next 50 years as shown next.

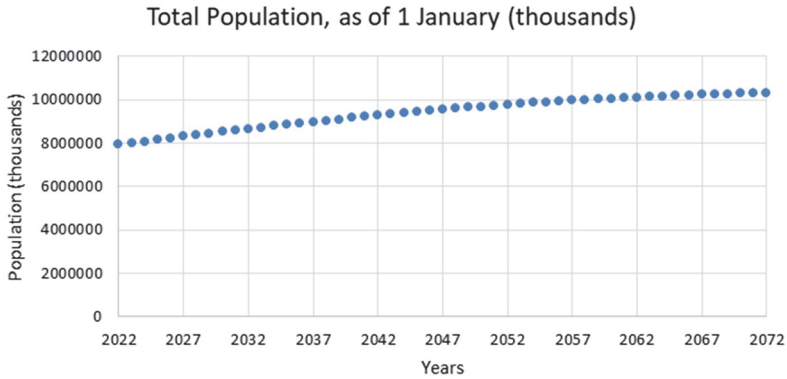


Figure 1: Extract of: World Population Prospects 2022 by UN, 2022.

Consequently, we believe that the utilization of electricity will continue to grow in the upcoming years.

Additionally, we can pay attention on how the electricity is being generated around the world, for example in the 38 OECD countries (Organisation for Economic Co-operation and Development Countries) most of the electricity is obtained from fossil fuel-based methods such as coal, gas, nuclear and oil as reported by the IEA, 2021 and shown below in figure 2.

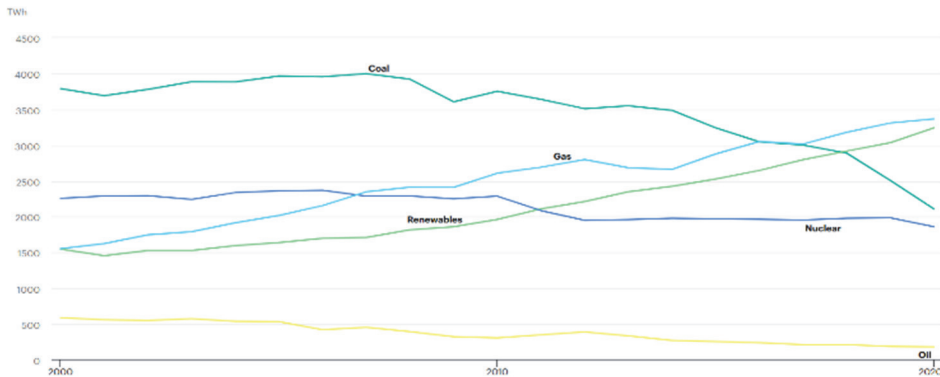


Figure 2: Electricity Generation by source, OECD, 2000-2020. From IEA, 2021.

It is noteworthy that the utilization of fossil fuels is declining: for instance, coal is rapidly diminishing by showing values from close to 4,000 TWh produced more than 15 years ago, to around half nowadays with values close to 2,100 TWh in 2020. Similarly nuclear sources appear to be slightly declining as well as oil utilization. The 2 sources that appear to be increasing are gas and the renewable sources as a whole category.

In regards of Kuwait, although not a direct member of the OECD, has been showing a trend of closer cooperation with them. For instance, in November 2023 Kuwait took part on the OECD

coordinated efforts regarding international tax-challenges (OECD, 2023), and in 2022 participated in the Global Forum on Transparency and Exchange of Information for Tax Purposes (OECD, 2022). Moreover, Kuwait shared their national plan “Smart Kuwait 2035” with the OECD in 2021 which provided feedback (OECD, 2021). These actions could be considered a signal of increased cooperation and shared knowledge. Hence, it may be reasonable to postulate that some of the parameters that are forecasted for OECD countries, could be applicable to Kuwait too in the future, namely the trend of increased utilization of renewable energy sources.

The increase in utilization of renewable energy sources around the world has many factors, and one them is the eventual depletion of world reserves in fossil fuels: Several models found in the literature concur in reaching a similar conclusion: that world reserves on fossil fuels are depleting and will continue to do so until their levels are so low that will render them impractical for electricity generation at mass scale. For instance, one of the works we refer to is the mathematical model presented by Shafiee. S. & Topal. E. in their 2009 paper, in which they estimate somewhat precise times of decreased availabilities for a variety of different fuel reserves. According to their work, oil availability is likely to decrease significantly in approximately 35 years (from their time of publication in 2009), coal for 107 years and gas for 37 years. This means that accounting for our current date makes it a correction of 20 years left for oil, 92 years for coal depletion and 22 years for gas depletion. Moreover, these findings concur with the model presented by Hubbert in 1956, which in turn is referenced by many sources and is often utilized by many scientists as a starting point when developing different depletion models of finite resources around the world, including fossil fuels.

Regarding the utilization of fossil fuels for electricity generation, we also pay attention to the data pertaining China as shown below in figure 3, from EIA, 2023.

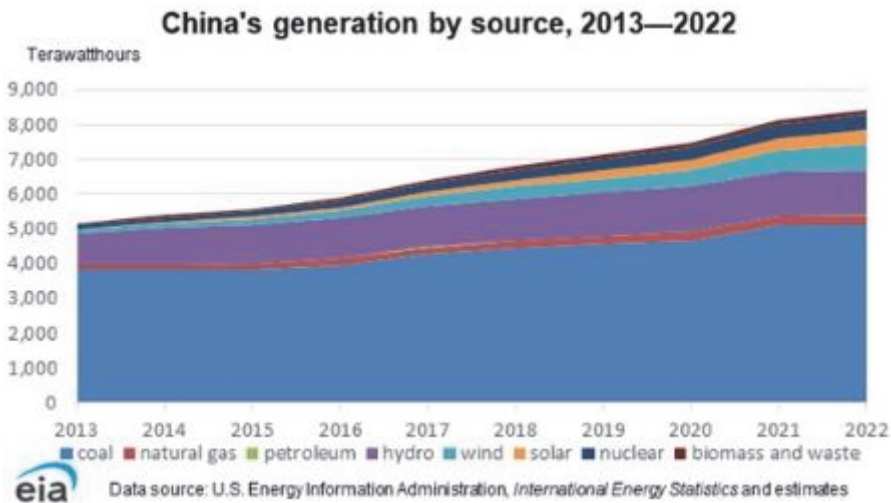


Figure 3: China's Electricity Generation by Source 2013-2022

It is noteworthy that although electricity generated from coal has increased from 3837 TWh in 2013 to 5144 TWh in 2022, the total demand has also increased, and as such the proportion of resource utilization increased at different levels with the renewable energy sources showing the most dramatic increases as shown next (EIA, 2013)

- Wind power generation increased by 24% from year 2021 to 2022.
- Solar generation increased by 22% from year 2021 to 2022.

- Hydropower generation increased 2% from 2021 to 2022.

The electricity statistics from China shown above could be considered as a key performance metric to understand the overall status of fossil fuels relationship to electricity generation, since China is currently ranked as the highest electricity consuming country of the planet, as shown in Figure 4 below (EIA, 2019).

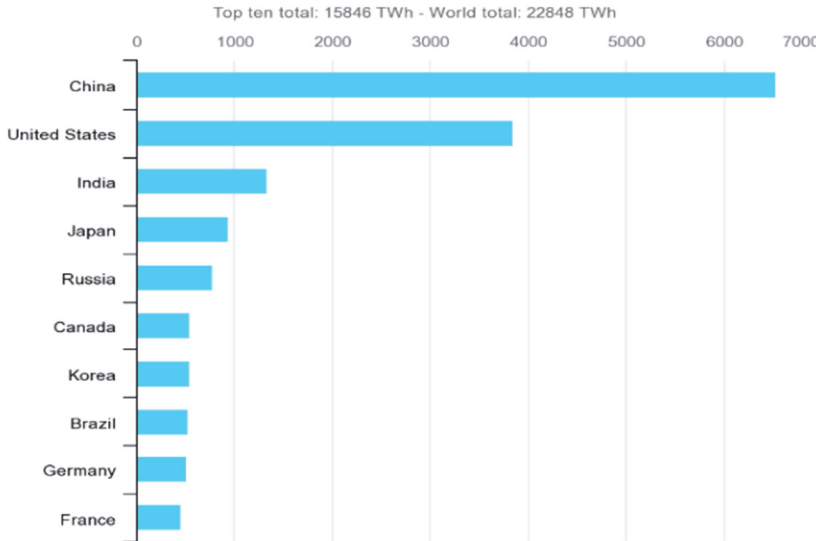


Figure 4: Top 10 electricity consuming countries, EIA, 2019.

From the discussions presented above we argue that electricity demand is currently increasing, and that the sources utilized to obtain it, are shifting from fossil fuels to renewable energy sources. As such, it is convenient for engineers and scientists around the world to collaborate in the study of renewable energy integration. Moreover, including high inflation rates to account for future possible economic scenarios.

2. Problem Statement

When designing electric networks and microgrids that will be utilized in the following years, the engineers should account for current world trends of resource shifting from fossil fuels to renewable sources, namely a Hybrid state in which both types of resources can co-exist during the shifting phase. Moreover, the inclusion of the renewable energy sources into a microgrid often requires the consideration of environmental factors when calculating the expected electric output of such components. Since environmental factors are probabilistic and randomized systems, there is an urgency to study alternative methods for hybrid microgrid configuration optimization and evaluation, such that a better understanding of these hybrid systems is enabled.

2.1 Objective and Value added

Our work explores the implementation of 3 stochastic optimization algorithms that are assembled to work in conjunction with a Montecarlo simulation, to allow an approximation of the optimal

configuration of a hybrid microgrid. The 3 algorithms under study are Genetic Algorithm, Fireworks Algorithm, and a new Hybrid Genetic-Firework Algorithm. These methods are compared and the results are analysed to provide recommendations regarding their utilization in the future. The programming language is Julia which is also considered a novel language.

2.2 Background

The subsequent definitions and ideas are developed based on our previously published work Lopez et al, 2023. The hybrid state of electric networks refers to the combination of different types of power generation and distribution systems. The transition from fossil fuel-based energy generation to renewable sources entails the implementation of hybrid electric networks, where both types of resources can coexist during an interim phase.

It is crucial to elucidate the distinction between power grid and micro grid. The electricity grid is typically owned by either the government or an electric utility business, and consists of three distinct stages: Electricity is generated, subsequently transmitted, and ultimately distributed to the end-users. The 3 steps operating together can be understood as the power grid.

Production Phase: The initial stage involves the generation of electricity. Power plants produce electricity on a large scale using various methods and sources. These sources can include fossil fuels like nuclear, coal, natural gas, and oil, as well as renewable sources like solar, wind, and hydro-power.

The second phase involves the transmission of electricity through a network specifically designed for this purpose. The transmission network are cable lines that convey the electricity from the power plants into the cities and towns where it will be used. Transmission lines typically operate at high voltages in order to minimise the losses associated with long distances.

Distribution step: The third step is the distribution phase, which usually takes place within urban areas. During this step, the voltage of the gearbox phase is reduced as a precautionary measure for safety reasons.

Microgrid: Upon reaching the private property, a distinct demarcation is often established at the electric metre to differentiate between the power grid and the micro grid. After the electric metre, the electric network becomes private property, and it is the duty of the end-user (property owner) to operate and maintain it securely, in accordance with the legal requirements and standards set by their country/state. The microgrid refers to the ultimate segment of the electric network that is privately owned.

2.3 Interconnected microgrids and isolated microgrids

Microgrids in urban areas are typically interconnected with the power grid, allowing end-users to directly purchase electricity from the electric company that generates it at their remote power plants, as previously mentioned. During these instances, the electric metre located at the border/connection between the micro-grid and power-grid is employed to quantify the quantity of electricity being supplied to the micro-grid. Consequently, the end-user is billed a predetermined monetary sum as stipulated in the contract between the end-user and the electric provider.

On the other hand, islanded microgrids are the private electric networks that are not connected to any provider. Consequently, it is the responsibility of the end-user to establish the connection of electricity-generating components, such as solar panels, wind turbines, diesel generators, and so forth.

2.4 Problem Formulation

We improve the economic analysis presented in Lopez et al, 2023 with the inclusion of the annual worth method (AW) as the basis for economical comparison between multiple mutually exclusive alternatives (MEAs), to provide the optimization algorithms with a more educated discernment

argument in situations where the microgrid components have different lifetimes. Additionally, the projection for future fuel prices is refined with the introduction of the Donchian channel approach as the basis to distinguish potential breakout levels in conjunction with a linear forecasting technique, that allows a projection of price onto the future when assuming strong inflation effects. Moreover, the electricity price that can be purchased via Power Grid is analysed for 134 countries for which an upper control limit is defined and used as a potential scenario level that could occur if these prices fall out of control during unexpected market situations. Other improvements presented in this work are the expansion of our problem formulation to include a connection to the power grid that allows the possibility of the hybrid microgrid to be islanded or connected; also, in this work the wind turbine's model is updated to use a power curve as a basis of electricity output estimations, and lastly, we put a maximum capacity to the Power Grid purchases per day, to represent potential rationalization of this resource in the future in case of severe hardships.

The inflation level utilized in this work remains the same as before, expressed at 7%, per annum for at least another decade.

The rest of the formulation continues similar to our previous work: the configuration of a hybrid microgrid is understood to be the list of components that are contributing electricity into the system, as well as the total electric demand of the system.

The electricity source components considered in our formulation are: Solar Panels, Wind Turbines, Diesel Generators, Electric Batteries, Converters which can be both Inverters and Rectifiers, and we include now a connection to the Power Grid.

Since our stochastic optimization methods will include a genetic algorithm, fireworks algorithm, and hybrid genetic-fireworks algorithm; we encode the configuration of the microgrid electricity sources as a sequence 'S' of potential values as follows:

$$S_1 = \{V_1, V_2, V_3, V_4, V_5, V_6, V_7\}$$

Where:

V_1 = Number of Solar Panels

V_2 = Number of Wind Turbines

V_3 = Number of Diesel Generators

V_4 = Number of Electric Batteries

V_5 = Number of Converters

V_6 = Connection to the Power Grid

V_7 = Annual Worth of the microgrid configuration

It is noteworthy that the values of V_1 to V_5 are integer values that are positive or greater than zero. However, the value of V_6 is binary representing 1 for 'Power Grid Connection Included' and 0 for 'Islanded Microgrid'. The value of V_7 is any real number since it represents the Annual Worth of the configuration as it will be evaluated by the Montecarlo simulation.

This means that our method in general can be described with the following diagram shown in figure 5:

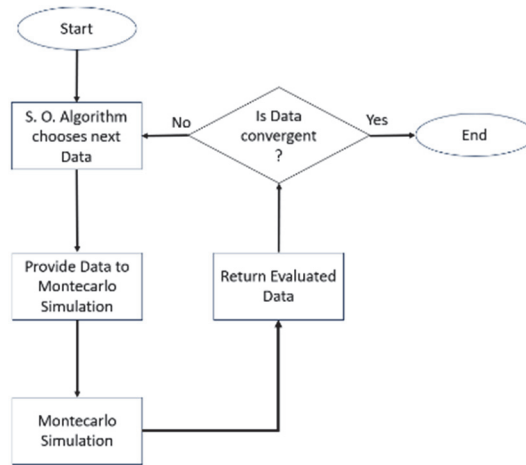


Figure 5: Stochastic Optimization General Flow Diagram

Where the Stochastic Optimization Algorithm (S.O. Algorithm) will perform its own process (discussed in next section) to decide which configuration to evaluate. Once it has been decided, the corresponding sequence i , $S_i = \{V_1, V_2, V_3, V_4, V_5, V_6, V_7\}$ will be sent to the Montecarlo simulation for evaluation, which in turn will return an answer (Annual Worth in our case) and store it in the value V_7 . In this way the Stochastic Optimization Algorithm has vision of the obtained value, which, in turn can be utilized to decide if another iteration is needed or a convergence criterion has been met. The algorithm objective is to maximize Annual Worth.

In other words, the Montecarlo simulation is used as a function f in the evaluation steps of the different stochastic optimization algorithms:

$$V_7 = f(V_1, V_2, V_3, V_4, V_5, V_6)$$

The list of components and how each is formulated is shown next:

2.5 Solar Panels

The solar panel model used is the one proposed by Lambert et al.

$$S(t)_{PVij} = Y_{PVij} f_{PVij} \left(\frac{G_T}{G_{T,STC}} \right) \left[1 + \alpha_{Pij} (T_{Cij} - T_{C,STC}) \right]$$

Where

Y_{PVij} = represents the rated capacity in kilowatts of the PV array i of size category j , and

f_{PVij} = represents the PV derating factor of the solar panel

G_T = represents the solar radiation at the present moment, measured in kilowatts per square metre (kW/m²).

$G_{T,STC}$ = represents the sun radiation measured under normal test circumstances.

α_{Pij} = represents the temperature coefficient of power for the solar panel.

T_C = represents the temperature at the present time step, measured in degrees Celsius

$T_{C,STC}$ = represents the temperature at standard test conditions, which is specifically defined as 25°C.

The aforementioned values can be acquired from the component supplier, with the exception of T_C and G_T , which must be gathered from environmental conditions specific to the microgrid's location.

2.6 Solar Irradiation

We write a sequence of 24 values that correspond to the solar irradiation hour by hour for a representative day of the geographical region under study. This means that we represent a vector V_{solar} as follows:

$$V_{solar} = \{R_1, R_2, R_3, \dots, R_{22}, R_{23}, R_{24}\}$$

Such that each value contained in R_1 to R_{24} is expressed in kW/m^2 for each hour of the day. Additionally, 2 values are defined: daily variability and hourly variability. The daily variability is used to randomly shift up or down the entire vector values as a group, to represent that some days are different from other days. The hourly variability is used to randomly and slightly shift up or down individual hourly values R_1 to R_{24} to represent that hourly irradiation can differ due to clouds, dust, or other factors.

$$Solar_{DailyVariability} = [0 \text{ to } 1]$$

The solar daily variability can take values between 0 and 1 as a percent change to be potentially allowed randomly for an entire day as a group.

$$Solar_{HourlyVariability} = [0 \text{ to } 1]$$

The solar hourly variability takes values between 0 and 1 to represent random percent change that can happen within the hours.

This formulation will allow the Montecarlo simulation to generate values representative of the weather of certain region. We recommend obtaining the solar irradiation from the NASA Prediction of Worldwide Energy Resource (POWER) database as it is quite complete and is available free online. We advise the reader to convert the irradiation from the database by dividing by 1,000 as the data is provided in W/m^2 but kW/m^2 are needed in the solar panel model adopted in this paper.

2.7 Wind Turbines

In this work we update our previous wind turbine model approach: in this version of our work, we do not use a formula per sé but a power curve is implemented to represent the electricity output when a given windspeed is present. The power curves for many wind turbines can be obtained from the manufacturer directly, however we utilize the data from a generic 65kW Wind Turbine as the basis, and scale it up or down depending on the rated output of the wind turbine we are modelling. The power curve used as a base is the following shown in table 1 obtained from the work of Faizan A. found on electricalacademia.com:

Table 1: 65kW Wind Turbine Power Curve

Power Output (kW)	0	0	0.7	2.2	6.5	13.8	22.7	32.1	41.3	46.5	52.8	58.7	61.7	62.9	63.8	64.7	63.5	62.6	61.7	61.2
Wind Speed (m/s)	2	3	4	5	6	7	8	9	10	11	12	13	14	15	16	17	18	19	20	21

From the data above, we can see that the maximum output for this power curve is obtained at 17m/s for an output of 64.7 kW. If we note that the rated output is 65 kW, we estimate a coefficient of performance of 0.99 and we this value in conjunction with scaling up or down the curve to represent wind turbines of different sizes.

Once a windspeed is present, then the electric output is obtained by linear interpolation using the closest values from the table, if the wind speed is bigger than 21 m/s the last value from the table is reported, and if the windspeed is smaller than 2 m/s the reported value is zero.

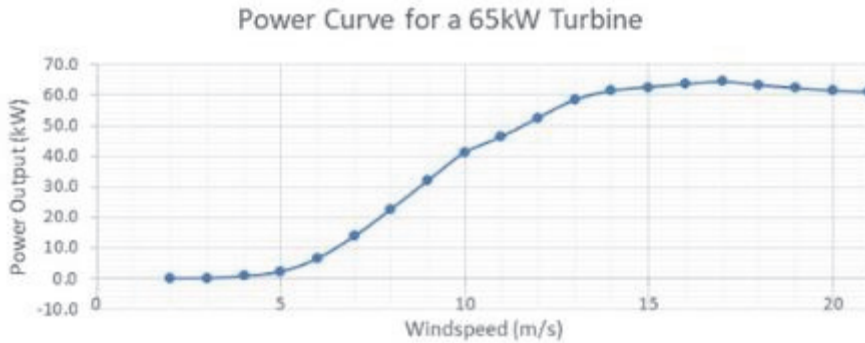


Figure 6: Power Curve for a 65kW Turbine, used as a basis for different sizes.

2.8 Windspeed

Similar to the solar irradiation, we write a vector of 24 values that correspond to the windspeed hour by hour for a representative day of the geographical region under study, as follows:

$$V_{wind} = \{Q_1, Q_2, Q_3, \dots, Q_{22}, Q_{23}, Q_{24}\}$$

Such that each value contained in Q_1 to Q_{24} is expressed in m/s for each hour of the day. Additionally, 2 values are defined: daily variability and hourly variability. In the same fashion as with solar irradiation, the daily variability is used to randomly shift up or down the entire vector values as a group, to represent that some days are different from other days, while the hourly variability is used to randomly shift up or down individual hourly values Q_1 to Q_{24} to represent that hourly windspeeds can differ due to humidity, temperature, or other factors.

$$Wind_{DailyVariability} = [0 \text{ to } 1]$$

And the wind daily variability can take a value between 0 and 1 to represent potential percent changes allowed randomly for an entire day as a group.

$$Wind_{HourlyVariability} = [0 \text{ to } 1]$$

The wind hourly variability can also take a value between 0 and 1, however this represents the random percent change that can happen within the hours.

2.9 Diesel Generator Model

The model for the electricity provided by the diesel generator is the following:

$$S(t)_{DGij} = P_{i,j} * efficiency_{i,j} * Level_{i,j}$$

Where:

$P_{i,j}$ = Rated output capacity of diesel generator i of size category j.

$efficiency_{i,j}$ = Efficiency of diesel generator i of size category j.

$Level_{i,j}$ = Is the level expressed as a percentage of maximum capacity at which the diesel generator i of size category j is currently operating.

Fuel utilization Model

The amount of fuel in liters utilized by the diesel generator i of size category j depends on the capacity of the generator itself as well as the level of operation at which the device is working at the moment, and lastly the efficiency is also considered.

$$L(t)_{DGij} = P_{i,j} * efficiency_{i,j} * Level_{i,j} * \frac{3.6}{(LHV\rho_{diesel})}$$

Where:

$P_{i,j}$ = Rated output capacity of diesel generator i of size category j .

$efficiency_{i,j}$ = Efficiency of diesel generator i of size category j .

$Level_{ij}$ = Is the level expressed as a percentage of maximum capacity at which the diesel generator i of size category j is currently operating.

LHV = Lower heating value of fuel, which is a metric of the energy contained in a kg of diesel measured in MJ/kg, in our case for diesel the value is = 43 MJ/kg

ρ_{diesel} = density of fuel, in our case diesel = 0.85 kg per liter.

2.10 Converters Model

The converters are modelled with an efficiency factor in the amount of electricity conversion as well as considering the maximum capacity of electricity that is convertible both from alternate current (AC) to direct current (DC) and vice versa. In our work we assume the same efficiency value can be used in both directions.

$$C_{ij}(t) = \begin{cases} Input(t) * Conv_{efficiency_{ij}} & \forall input(t) < Capacity \\ Capacity * Conv_{efficiency_{ij}} & \forall input(t) \geq Capacity \end{cases}$$

Where:

$Input(t)$ = The summation of electricity to be converted at time t

$Capacity$ = Capacity of 1 converter multiplied by the number of converters, which is contained in V_5 of equation 1.

This means that if the electricity available for conversion is more than the installed capacity in converters at any given time t , only the maximum capacity amount will be converted and the rest will be wasted.

2.11 Electric Battery Model

The electric battery reacts when there is need of more electricity (pull from available stored) or when there is excess electricity (push into the battery). Hence the expression is:

$$EB(t)_{ij} = \begin{cases} EB(t-1)_{ij} * D_{ij} + b_p(t) * C_{in_{ij}}, \forall b_p(t) > 0 \\ EB(t-1)_{ij} * D_{ij}, \forall b_p(t) = 0 \\ EB(t-1)_{ij} * D_{ij} - b_p(t) * C_{out_{ij}}, \forall b_p(t) < 0 \end{cases}$$

Where:

$EB(t)_{B_{ij}}$ = represents the amount of power stored in kilowatt-hours (kWh) at the current time step.

$EB(t-1)_{B_{ij}}$ = represents the amount of power, measured in kilowatt-hours (kWh), that was stored in the preceding time step.

D_{ij} = represents the depletion factor that occurs when the electricity remains stored.

$b_p(t)$ = represents the partial electric balance at the current time step.

The variable $C_{in_{ij}}$ represents the efficiency of the process of transferring electricity into a battery.

The variable $C_{out_{ij}}$ represents the efficiency of extracting electricity from the battery.

Lastly, the incomplete electric equilibrium $b_p(t)$, refers to the aggregate electrical generation generated by the aforementioned components.

2.12 Fuel Price Model

The fuel price is forecasted for the future years based on the Donchian channels approach inspired in the work of Swart J.N., 2016. The Donchian channel indicator is plotted on the monthly prices of light crude oil chart of the last 9 years of historical data as reported by the broker ActivTrades shown next

in figure 7:



Figure 7: Light Crude Oil monthly prices with Donchian Channel indicator and Stochastic Indicator

The upper diagonal yellow line depicts the value at which the Donchian channel was hit 9 years ago (January 2015) since that point could be considered a singularity, and a line starting from said point is expanded diagonally upwards onto the future by passing over the higher price limit that is marked by the upper horizontal yellow line, and could be considered a traditional price resistance. Then, the lower diagonal yellow line is defined from the point of another singularity that could be defined on April 2020 and expanded diagonally upward by passing below the support-resistance level found at approximately 74.45, since this level acted as resistance from periods of 2019 and before, and appears to be showing signs of support nowadays. Consequently, a channel is created between the 2 yellow diagonals shown on figure 7 above.

From the 2 diagonal lines shown above we mark the price of light crude oil on January 1st 2015, with a price of 46.66 USD per barrel, as well as the price reported on January 1st 2024 of 71.39 USD per barrel. These prices are used to estimate a slope $m=2.7477$ increment per year. Consequently, by using linear forecasting this behaviour yields a price of 98.86 USD per barrel in 10 years from now, and this is assuming the price will be on the upper limit of the defined channel range. This represents an increment of 38.49% of the current price.

In the same fashion, the price of diesel per gallon is found at the same time for 1.68 USD per gallon for the old price and 2.28 USD per gallon for the new price, which converting to liters gives 6.3594 USD per liter and 8.6307 for old and new price respectively, yielding a slope $m=0.2523$ per year. Following the same process, we estimate that a price of 11.1543 USD per liter of diesel could be assumed for the future price 10 years from now if the upper limit channel is hit in the next decade. This would represent an increment of 29.24%.

Since this analysis infers that the price of diesel could be increasing over the next years, a simplification of this behaviour is defined as expressing the price increases as a gradient series in a Cash Flow Diagram (CFD) as shown next in figure 8:

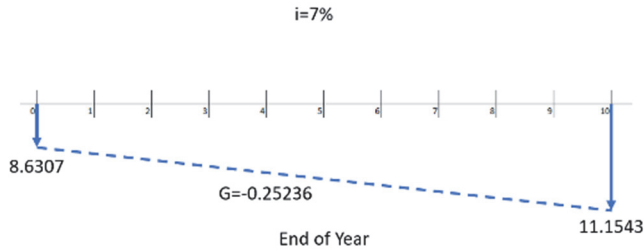


Figure 8: Gradient series for diesel price during the following 10 years

The cashflows in figure 8 point down as the engineering economics convention defines these as costs, and the interest rate is set at 7% to assume a high inflation rate environment. This series is used to yearly estimate the price of fuel when estimating Annual Worth.

Additionally, the collection of electrical components that are using power is consolidated under a single comprehensive term, referred to as total demand at time t : $TD(t)$. This term represents the overall amount of electricity being consumed in the microgrid at any given moment, achieved by combining the power usage of all electrical devices such as lightbulbs, ventilation systems, screens, and others.

2.13 Blackout Penalties

When the total demand exceeds the total available electricity, we incur on a blackout, and for each blackout we define a large monetary penalty to discourage this behaviour during the optimization process of the stochastic algorithms. A penalty is implemented each time t that electricity supply is non-sufficient to satisfy the microgrid electric demand.

2.14 Grid Connection

When a blackout is about to be incurred, electricity can be purchased from the power grid if this connection is available. The connection to the power grid also has a maximum capacity, consequently if this limit is exceeded then the blackout proceeds. This capacity represents potential future rationalization of the resource of electricity on harsh situations that may derive if there is a pronounced shortage of fuel on the future.

2.15 Purchased electricity price

The price of electricity is set at the upper control limit of 3 standard deviations from the average purchasing price of electricity of 134 countries as obtained from globalpetrolprices.com

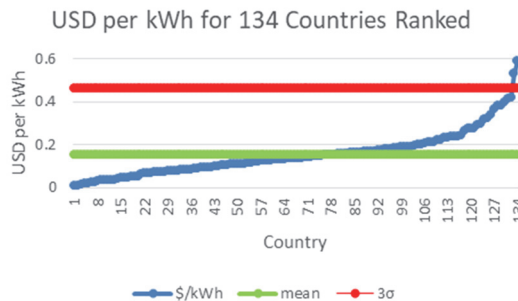


Figure 9: Electricity cost per kWh of 134 with average and 3σ upper level

The average purchase price is found to be 0.153 USD per kWh and the mean absolute deviation used as an approximator of the standard deviation, is found to be 0.102 USD per kWh. This yields a cost of electricity as follows:

$$Electricity_{cost} = 0.153 * 3(0.102) = 0.461 \text{ USD per kWh}$$

We use this value to assume an increment of electricity cost during the upcoming decade as the worst-case scenario, that may reach to out-of-control limits.

2.16 Annual Worth Formulation for Objective Function

From the above we can present the formulation of our objective function: the Annual Worth. The annual worth can be understood as the annualized equivalent payment of a cashflow when considering the effect of compounding interest rates. We calculate the total cost of implementing each component into our microgrid as follows, and calculate the total annual equivalency for each, and add all values together in a single term that is then used as the target of optimization. At this point is evident that the objective is to minimize Annual Worth.

The objective function can be described as follows:

$$Min(AW) = AW_{V1} + AW_{V2} + AW_{V3} + AW_{V4} + AW_{V5} + AW_{V6}$$

Where:

AW = Total annual worth

AW_{V1} = Total annual worth of Solar Panels

AW_{V2} = Total annual worth of Wind Turbines

$AW_{V3} = AW_{DG} + AW_{Fuel}$: Total annual worth of diesel generators + annual worth of fuel purchased

AW_{V4} = Total annual worth of electric batteries

AW_{V5} = Total annual worth of converters

$AW_{V6} = AW_{Grid} + AW_{Penalties} + AW_{PurchasedElectricity}$: Total annual worth of Power Grid Connection + annual worth of penalties + annual worth of electricity purchased

The cost formulation presented above does not include any revenue, as it represents a micro-grid that is **not selling** any electricity back to the power grid.

Moreover, please note that the total annual worth of fuel cost, electricity purchased and blackout penalties are included in the component their related components V_3 for fuel as it relates to diesel generators, blackout penalties to V_6 as this pertains to the power grid connection as well as the annual worth of electricity.

2.17 Annual Worth of Solar Panels

The annual worth of solar panels is calculated as the annual worth of a single solar panel and multiplied by the number of solar panels. In order to calculate this amount, we include the initial cost, annual maintenance and operation costs as well as a salvage value at the end of the useful lifetime for a single solar panel, in the fashion of the cashflow diagram shown below:

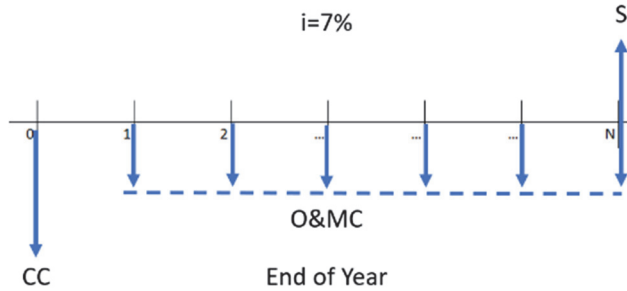


Figure 9: Solar Panel Cashflow diagram

In the diagram from figure 9, CC stands for capital cost which is the cost of initial purchase, initial transportation, installation costs as well as any other cost associated with obtaining the item until the component is connected and running correctly within our microgrid. This includes any licensing fee, permits, etc. Additionally, the O&MC stands for the yearly operation and maintenance costs incurred in keeping the device operational during the year, and the S stands for any salvage value that we may recover at the end of the component's useful life at year N, in which the item may be sold or scrapped. The interest rate is set in our paper to 7% to accommodate for an aggressive level of inflation type of scenario.

The method to calculate annual worth from the cashflow diagram shown above in figure 9 is clearly explained in the textbook by W. Sullivan et al, 2014. From which the following approach is presented:

$$AW_{V_1} = V_1 \left(-CC \left(\frac{A}{P}, i, N \right) + S \left(\frac{A}{F}, i, N \right) - O\&MC \right)$$

Where:

AW_{V_1} = Annual worth of solar panels

V_1 = Number of solar panels

CC = Capital cost

S = Salvage value

O&MC = Yearly operation and maintenance costs

$(A/P, i, N)$ = Is the functional symbol of the factor "A given P" to find the equivalent uniform annual series of payments during N years for a cashflow occurring in present time that is subjected to a compound interest rate i , as defined by engineering economics conventions as follows:

$$(A/P, i, N) = \frac{i(1+i)^N}{(1+i)^N - 1}$$

$(A/F, i, N)$ = Is the functional symbol of the factor "A given F" to find the equivalent uniform annual series of payments during N years for a cashflow occurring in the future time at year N and is subjected to a compound interest rate i , as defined by engineering economics conventions:

$$(A/F, i, N) = \frac{i}{(1+i)^N - 1}$$

2.18 Annual Worth of Wind Turbines, Diesel Generator, Electric Batteries, Converters, and Power Grid Connection

The calculation of the annual worth of wind turbines follows the same structure as for the solar panels but updating the corresponding values for V_2 = Number of wind turbines, the Capital Cost (CC), Operation and Maintenance Costs (O&MC), Salvage value (S) and lifetime in years (N), such as to accurately represent the wind turbine costs.

And the rest of the components follow a similar process, but updating the values

correspondingly.

2.19 Annual Worth of Fuel Utilization

The annual worth of the amount of fuel purchased is the amount of fuel purchased yearly multiplied by the cost of fuel which is increasing in a gradient fashion as shown in figure 8 previously shown. Hence the uniform annual equivalent cost from the gradient behaviour is given by:

$$AW_{Fuel} = \sum_{t=1}^{8760} L(t)_{DGij} (-8.6307) - 0.25236 \left(\frac{A}{G}, i, N \right)$$

Where:

AW_{Fuel} = The annual worth of the purchased fuel

$\sum_{t=1}^{8760} L(t)_{DGij}$ = Is the summation of the purchased fuel, hour by hour during a full year

The value 8.6307 is the current cost of fuel as shown in figure 8 shown before

The value 0.25236 is the gradient representative of price increase as shown in figure 8 before

$(A/G, i, N)$ = Is the functional symbol of the factor "A given G" to find the equivalent uniform annual series of payments during N years for a cashflow occurring in a recurrent manner and which are increasing linearly by an amount G each year, until a future time at year N, and are subjected to a compound interest rate i, as defined by the engineering economics conventions as follows:

$$(A/G, i, N) = \frac{1}{i} + \frac{N}{(1+i)^N - 1}$$

2.20 Annual Worth of Blackout Penalties

Each time there is not enough electricity, a penalty is incurred. The annual worth of such penalties is just the summation of penalties incurred on a given year multiplied by the penalty cost:

$$AW_{penalties} = PenaltiesPerYear * CostOfPenalty$$

2.21 Annual Worth of Purchsed Electricity

The amount of purchased electricity is added in a cumulative fashion hour by hour, to find the total amount purchased per year, and this amount is multiplied by the cost of electricity. The cost of electricity is set as the higher control limit of a 3-sigma level located above the average price of several countries, yielding a cost of 0.461 per kWh as shown in equation 13, to have a worst-case scenario representation of projected economic hardships.

$$AW_{PurchasedElectricity} = \sum_{t=1}^{8760} Purchase(t) (-0.461)$$

3. Methodology

The system is evaluated using a Monte-Carlo simulation that works as a black box that finds the Total Annual Worth of any microgrid configuration that is sent by the stochastic optimization algorithms. The method implementation is inspired by the discussions provided in the book by Sobol I. M. 2017. The formulation of the Montecarlo simulation is adapted from our previous work to encompass the inclusions mentioned above, from where the steps are the following:

Step 1: Calculate the environmental factors for solar irradiation and wind speed using the methods described previously in this paper.

Step 2: Calculate individual electrical contributions of each component as these depend on their corresponding environmental weather conditions estimated in step 1, and considering their individual parameters.

Step 3: Summation of all electricity production contributions into a single value.

Step 4: Update battery storage system by degrading the value stored from the previous hour, by using the factor of storage efficiency.

Step 5: Decision making: if the electricity produced is more than needed, push excess into batteries. If electricity produced is less than needed, pull the remaining from the battery.

Step 6: Update the amount of electricity being stored/pulled from batteries by introducing losses considering the capacity and efficiency of the installed converters.

Step 7: Decision making: if the electricity needs to be pulled from the battery and there is not enough in storage incur in a blackout penalty.

Step 8: Decision making: if there is a blackout penalty try to purchase the needed amount from the power grid, when the power grid is available.

Step 9: Decision making: if purchasing the needed amount from the power grid satisfies the demand, cancel the blackout as non-existent, if the purchase did not solve the issue, keep the blackout penalty.

Step 10: Repeat the process until simulation is completed.

Step 11: Calculate annual worth using the obtained values for electricity purchased and blackouts incurred.

3.1 Optimization with Genetic Algorithm

The first stochastic optimization method used in this paper to find a microgrid configuration is the genetic algorithm, which is a method that approximates the solution to an optimization problem by means of evolutionary theory and has been widely utilized world-wide such as the work of M.S. Ismail et al in 2014 where a genetic algorithm is used to model and design hybrid renewable energy systems, or the work of M. J. Mayer et al in 2020 where it is used in similar fashion however is expanded to utilize multi-objective optimization. As it pertains our formulation, the genetic algorithm is performing single objective optimization by maximizing the annual worth (AW) of several available combinations that exist to configure a microgrid.

The implementation of the genetic algorithm in our work is presented with the following parameters:

- Population size = 100
- Convergence = 50 iterations without improvement
- Elite = top 10%
- Mutation = 25%
- Maximum number of iterations = 1000
- Reproduction Method = Roulette with non-repetition

Search space:

- Maximum Number of Solar Panels = 100
- Maximum Number of Wind Turbines = 100
- Maximum Number of Diesel Generators = 100
- Maximum Number of Electric Batteries = 100
- Maximum Number of Converters = 100
- Maximum Number of Power Grid Connections = 1

The Chromosome is encoded according to the structure outlined in equation 1 of this paper, and it was implemented as follows:

First step - Initialization: Generate a population of $N=100$ chromosomes, where each gene is assigned a random value within the specified bounds.

Step 2 - Assessment using Monte-Carlo Simulation: The Monte-Carlo simulation is performed on each chromosome to determine the overall yearly value.

Step 3 - Evaluating the answers in order of importance: The population is ranked based on their total annual value, with the highest ranked as the best and the lowest ranked as the worst.

Step 4 - Elite identification: The most exceptional chromosomes are recognised and automatically preserved for the future generation.

Step 5 - Verify convergence and terminate if necessary: If the alpha individual remains unchanged from the previous generation, increment a counter. Terminate if this counter surpasses the convergence threshold.

Step 6 - Non-repetitive roulette reproduction: The people with higher rankings have a greater chance of being chosen for reproduction, whereas those with lower rankings have a reduced chance of being chosen. Subsequently, a stochastic number is generated to designate 2 chromosomes for the purpose of reproduction. These selected chromosomes then produce 2 progeny by merging their respective gene values. Once chosen for reproduction, the two parents are excluded from the population to ensure they are not selected again. This process is iterated until the offspring produced reaches the population size minus the elite fraction.

Step 7 - Mutation: Randomly selected individuals among the progeny undergo the process of mutation, when a random gene is altered to a random value.

Step 8 - Iterate: We commence the subsequent iteration from step 2.

The outcomes derived from this methodology are subsequently contrasted with those achieved using the fireworks algorithm and subsequently with the hybrid genetic-fireworks algorithm.

3.2 Fireworks algorithm

The fireworks algorithm approximates the optimal by implementing an iterative approach, in which the combinations are represented by a sequence of values called sparks.

The fireworks algorithm has been used successfully in previous projects pertaining to microgrids, such as the work of Jadoun et al in 2018 in which they use it to manage various dynamic loads on a microgrid by taking advantage of the method's high adaptability, or the work by Want et al in 2017 in where they optimize the microgrid merely by fireworks algorithm, among others. The parameters of the fireworks algorithm employed are the following:

- Population size = 100
- Explosion Amplitude = each firework produces 3 new individuals in the neighborhood.
- Explosion Interval = Each generation.
- Spark range = Ranked box percentage of total range for each gene.
- Convergence = 50 iterations without improvement.

The firework algorithm is encoded as shown in equation 1 of this paper, and the search space is the same as for the genetic algorithm:

- Maximum Number of Solar Panels = 100
- Maximum Number of Wind Turbines = 100
- Maximum Number of Diesel Generators = 100
- Maximum Number of Electric Batteries = 100
- Maximum Number of Converters = 100
- Maximum Number of Power Grid Connections = 1

The firework algorithm is implemented as follows:

The initial phase is the initialization process. Create a population of 100 fireworks, where each spark exhibits a randomly chosen value within the given parameters.

Step 2 - Assessment utilising Monte-Carlo Simulation: Every firework successfully undergoes the Monte-Carlo simulation to determine its annual value.

Step 3 - Assessing and ranking the solutions: The population is ranked in descending order according to their highest annual worth.

Step 4 - Confirm convergence and terminate if required: Confirm if the alpha individual matches the preceding generation, and decide whether to continue or end the process in a manner akin to step 5 of the genetic process.

Step 5 - Reducing Population: Selecting the top N individuals from the population while maintaining a stable population size over the iterations. This stage is crucial because each firework

will generate offspring fireworks, leading to a temporary increase in the population size. The fireworks from the previous iteration will remain in the population unless they are ranked outside the top N individuals.

Step 5 - Allocate box ranges: The ranks are assigned consecutive box ranges, spanning from 1% to 100%. Individuals with higher ranks are assigned a tighter range of sparks, whilst those with lower ranks are assigned a broader range of 100%. In this example, the population size is set at 100. Consequently, each firework has a linear rise in their box range, starting from 1% at the highest point and reaching 100% at the lowest point.

Step 6 - Detonations: In our scenario, each firework will generate three additional fireworks by generating random spark values within the specified range. This means that the new spark values will be calculated by adding or subtracting a percentage of the existing spark value. This process will generate novel fireworks that closely resemble the original values for individuals with good performance, while gradually diverging from the original for individuals with low rankings. This allows for a balance between exploiting the existing knowledge and exploring new possibilities.

Step 7 - Iteration: We commence the subsequent cycle starting from step 2.

3.3 Hybrid Genetic-Fireworks Algorithm

The novel hybrid Genetic-Fireworks algorithm tries to combine the working principles of both the genetic algorithm and the fireworks algorithm, such as the work presented by Łapa K. & Cpałka K. in 2016 in which they use it to select parameters regarding the structure of controllers, in our work we adapt it to help select the best microgrid configuration with the aid of the Monte Carlo simulation explained above.

The implementation of the hybrid genetic-fireworks algorithm is implemented with the following parameters:

- Population Size = 100
- Iterations for Convergence = 50
- Maximum iterations = 1000
- Elite Fraction = 0.10
- Mutation Fraction = 0.25
- Explosion Amplitude = 3, means that each firework produces 3 new individuals in the neighbourhood

The hybrid genetic-fireworks algorithm is encoded as shown in equation 1 of this paper, and the search space is the same as for the genetic algorithm and the fireworks algorithm:

- Maximum Number of Solar Panels = 100
- Maximum Number of Wind Turbines = 100
- Maximum Number of Diesel Generators = 100
- Maximum Number of Electric Batteries = 100
- Maximum Number of Converters = 100
- Maximum Number of Power Grid Connections = 1

The implementation of the hybrid genetic-fireworks algorithm is as follows:

First step - Initialization: Generate a population of $N=100$ chromosomes, where each gene exhibits a random value within the specified bounds.

Step 2 involves conducting an evaluation using Monte-Carlo simulation. The Monte-Carlo simulation is performed on each chromosome to determine its annual value.

Step 3 - Evaluating and prioritising the solutions: The population is rated based on their maximum annual wealth, from highest to lowest.

Step 4 - Verify convergence and terminate if necessary: Determine if the alpha individual is identical to the previous generation, and make a decision to either continue or terminate the process in a manner similar to step 5 of the genetic algorithm.

Step 5 – Population Trimming: Selecting only the top N people to form the population, while keeping the population size consistent across the iterations. This stage is essential because the hybrid genetic-fireworks algorithm generates extra chromosomes through the reproduction process of a genetic algorithm and also creates new chromosomes through the explosion process of the fireworks algorithm.

Step 6 – Genetic Reproduction Process: The population that has been trimmed goes through a reproduction process that follows the same methodology as outlined in the genetic algorithm implementation described in this paper. This process results in the creation of a population of chromosomes that are the offspring of the original population.

Step 7 – Mutation: The population of offspring undergoes a mutation process that is identical to the one employed in the genetic algorithm described in this research.

Step 8 – Firework explosions: The reduced population from step 6 undergoes the explosion process, which is similar to the one described in the fireworks algorithm published in this study.

Step 9 – Population concatenation: The population is combined to include the initial trimmed population of chromosomes, along with the children population and the population generated following the explosion process. The current population exceeds the initial population size.

Step 7 - Iteration: We commence the subsequent cycle from step 2.

4. Case Study

Certain residential property located in Kuwait has the following data:

- Home size = 5 person home
- Average kWh usage per day (kWh/Day) = 39.53 kWh per day
- The utilization climatization load: 31.70% of the daily load is due to climatization system utilization.

The daily electric demand of a representative day is shown as follows in table 1:

Table 1: Hourly demand of microgrid for a representative day

Hour	1	2	3	4	5	6	7	8	9	10	11	12
kWh	0.877	0.877	0.877	0.877	0.877	1.659	1.936	2.212	1.936	1.659	1.659	1.659
Hour	13	14	15	16	17	18	19	20	21	22	23	24
kWh	1.659	1.936	1.936	1.659	1.936	2.766	2.212	2.212	1.936	1.936	1.659	0.877

And this data can be shown graphically yielding the following electric demand curve shown in figure 10:

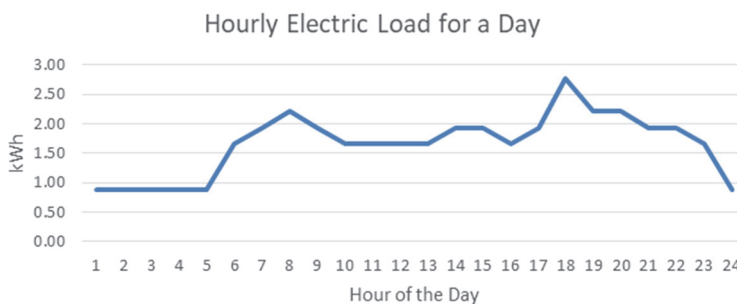


Figure 10: Electric hourly demand curve for a representative day

The daily demand randomness is set to $\pm 5\%$, while the hourly demand randomness is set to $\pm 15\%$. The solar irradiation for the region as well as the data regarding windspeed are obtained from the NASA Prediction of Worldwide Energy Resource (POWER) database. The data regarding windspeed is shown in table 2 next:

Table 2: Hourly Windspeed of a representative day in Kuwait

Hour	1	2	3	4	5	6	7	8	9	10	11	12
m/s	8.94	8.99	8.75	8.49	8.25	8.01	8.48	9.19	10.5	10.3	9.77	9.17
Hour	13	14	15	16	17	18	19	20	21	22	23	24
m/s	8.35	7.49	6.87	6.57	6.32	5.18	5.22	6.05	6.78	7.3	7.61	7.69

This data yields the following windspeed curve shown in figure 11:

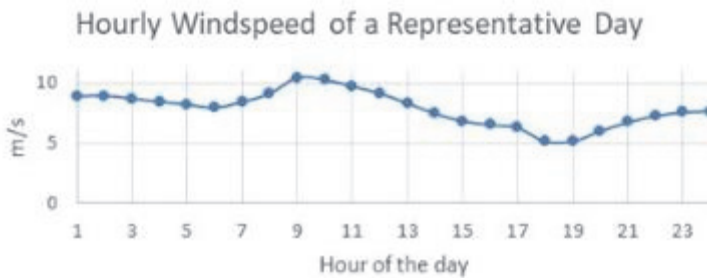


Figure 11: Hourly windspeed in the region for a representative day

The daily randomness for windspeed is set to $\pm 5\%$, and the hourly windspeed randomness is set to $\pm 15\%$.

The solar irradiation for a given representative day of the region is the following:

Table 3: Hourly solar irradiation for a representative day

Hour	1	2	3	4	5	6	7	8	9	10	11	12
$\frac{kWh}{m^2}$	0	0	0	0	0	0	0.229	0.550	0.715	0.805	0.848	0.780
Hour	13	14	15	16	17	18	19	20	21	22	23	24
$\frac{kWh}{m^2}$	0.750	0.689	0.561	0.396	0.234	0.026	0	0	0	0	0	0

And the daily solar irradiation randomness set to $\pm 5\%$, while the hourly solar irradiation randomness is set to $\pm 15\%$.

The components considered for inclusion in the microgrid are the following:

4.1 Solar panels

The solar panels considered have the following economic parameters:

- Solar Panel Capital Cost = 1,150 USD
- Solar Panel Annual Maintenance Cost = 300 USD
- Solar Panel Salvage Value = 0

- Solar Panel Life Time = 20 years
- And the following manufacturing parameters:
- Rated capacity = 0.415 kW
 - Derating factor = 19%, efficiency values are typically between 15% to 22% and the extreme highs up to 26%
 - Solar Irradiation at Standard Test Conditions = $1 \frac{kW}{m^2}$, this value is constant for most solar panels.
 - Temperature Coefficient of Solar Panel = 0, we set this value to simplify the model by neglecting the effect of temperature on the performance.
 - Temperature at current timestep = 32 Celsius, in our model we simplify this parameter and use a flat value for all timesteps, since the coefficient of temperature is set as 0.
 - Temperature at Standard Test Conditions = 25 Celsius, this value is constant for most solar panels.

4.2 Wind Turbines

The wind turbines considered have the following economic properties:

- Wind Turbine Capital Cost = 390,000 USD
- Wind Turbine Annual Maintenance Cost = 2,500 USD
- Wind Turbine Salvage Value = 2000 USD
- Wind Turbine Life Time = 15 years

With the following manufacturing properties:

- Wind Turbine Rated Output = 3 kW

4.3 Diesel Generators

The economical parameters for the diesel generator are the following:

- Diesel Generator Capital Cost = 3547.62 USD
- Diesel Generator Annual Maintenance Cost = 350 USD
- Diesel Generator Salvage Value = 20 USD
- Diesel Generator Life Time = 10 years

The manufacturer properties of the diesel generator are the following:

- Diesel Generator Rated Capacity = 5kW
- Diesel Generator Efficiency = 80%
- Diesel Generator Running at Standby Level = 70%, this value represents at what value of the maximum capacity is the diesel generator running, usually values between 70% to 80% are recommended by Caterpillar manuals.
- LHV of fuel = 43 MJ per kg, this value is a constant for diesel.
- Density of fuel = 0.85 kg per liter, this value is a constant for diesel.

4.4 Electric Batteries

The electric batteries have the following economical parameters:

- Battery Capital Cost = 156 USD
- Battery Annual Maintenance Cost = 0
- Battery Salvage Value = 0
- Battery Life Time = 12 years

The manufacturer properties of the electric batteries are the following:

- Battery Hourly Storage Efficiency = 99.99%

- Battery Capacity = 1 kWh

4.5 Converters

The converters have the following economical parameters:

- Converter Capital Cost = 131.06 USD
- Converter Annual Maintenance Cost = 0
- Converter Salvage Value = 0
- Converter Life Time = 15 years

And the manufacturer properties of the converters are the following:

- Converter Capacity = 120 kW
- Converter Efficiency = 90%

4.6 Power Grid Connection

The power grid connection has the following economical parameters:

- Power Grid Installation Cost = 0, when a power grid is creating a new contract for a new connection the value may not be 0, however if the connection is already present, then the 0 may be used.
- Power Grid Annual Maintenance Cost = 0
- Power Grid De-Installation Cost = 0, this value represents the analogous of salvage value, however instead of a revenue occurring at the end of the cashflow diagram, another cost may be incurred.
- Power Grid Contract Length = 5 years, this value is used as the lifetime of the component.

Additionally, the power grid has the following operational properties:

- Power Grid Maximum Capacity per Hour = 2.2 kWh, this value represents a top value over which electricity cannot be purchased during the same hour, in a residential region, for any other reason whatsoever, for example a potential rationalization of the electricity resource by some legal authority in case hard austerity measures may be implemented, or by the standard breaker circuits installed on the property to inhibit from excessive use of electricity.

5. Results

From the definitions mentioned before, the 3 stochastic algorithms are encoded in Julia language and the results are shown next.

5.1 Genetic Algorithm Results

The genetic algorithm yielded the following recommended solution:

- Recommended Number of Solar Panels: 39
- Recommended Number of Wind Turbines: 1
- Recommended Number of Diesel Generators: 0
- Recommended Number of Electric Batteries: 16
- Recommended Number of Converters: 1
- Recommended Connection to Power Grid: Yes
- Total Annual Worth = -4'061,761.925 USD

The convergence is found after 217 generations, with the following distribution of improvement along the generations:



Figure 12: Evolution of alpha chromosome ‘champion’

From the figure 12 above we notice great improvement on the first 20 generations after which the improvement was stable until convergence.

The yielded solution shows the following properties:

Regarding the annual electric demand distribution, a graphical representation is the following sequence of stripes showing red for higher values in demand and blue for lower levels in demand while green for intermediate levels of demand. This graphical representation is inspired by the HOMER software developed by NREL. There are 365 vertical stripes to represent each day of a year, and each stripe consists of 24 values to represent the hourly values during each day.

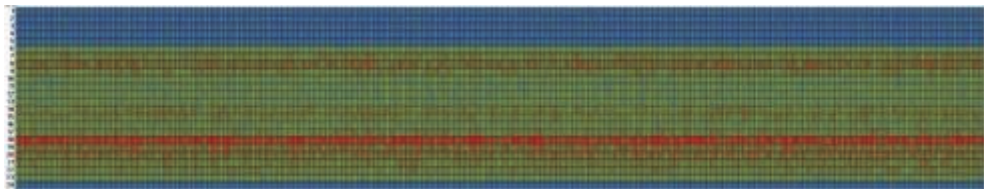


Figure 13: Hourly electric demand for an entire year

We notice the higher demand levels usually happening by the 18 hour of the day, and low levels of electric demand from hour 24 to hour 5 of the next day.

Next, we show the average electric demand that occurred per day for an entire year:

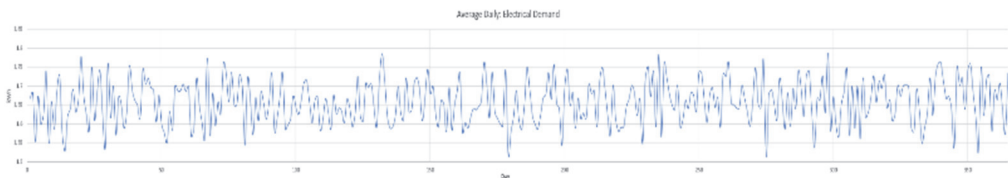


Figure 14: Daily demand averages for an entire year

The graph in figure 14 shows that the average level of demand varied differently from day to day as expected.

The stripe graph shown below in figure 15 shows the solar panel output behaviour each hour for the duration of an entire year, in similar fashion as in figure 14:

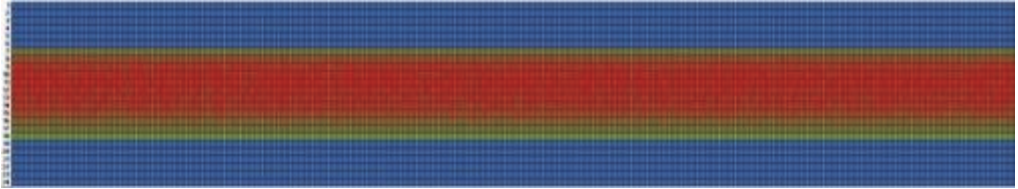


Figure 15: Hourly solar panels electric contribution for an entire year

We also show the daily average of electricity provided by the solar panels for an entire year in figure 16:

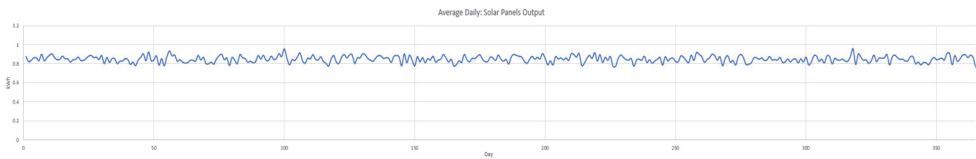


Figure 16: Daily solar panels contribution averages for an entire year

We see the pattern of the amount of electricity provided by the wind turbines in the graph below following the same structure as for the other components shown above.

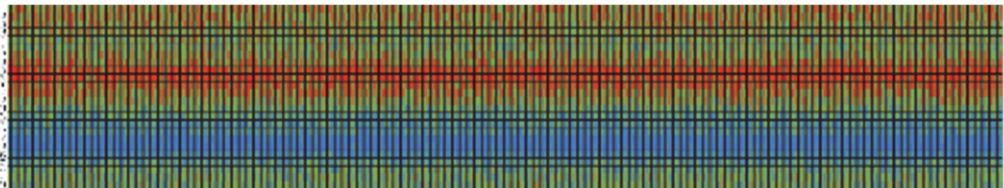


Figure 17: Hourly wind turbines contribution for an entire year

Next, we see the daily average contributions of wind turbines for an entire year:

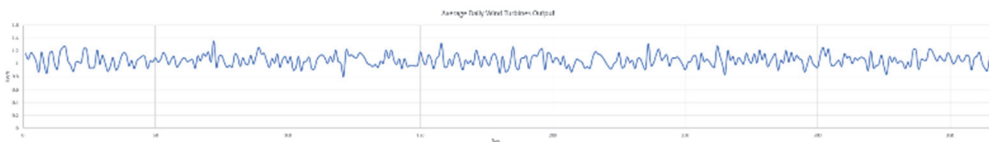


Figure 18: Daily wind turbines contribution averages for an entire year

Consecutively, the hourly contributions of diesel generators for an entire year are the following:



Figure 19: Hourly diesel generators contribution for an entire year

The values shown are all red since there is no contribution from diesel generators and all values are zero. Next the corresponding daily averages are also zero as shown in figure 20:

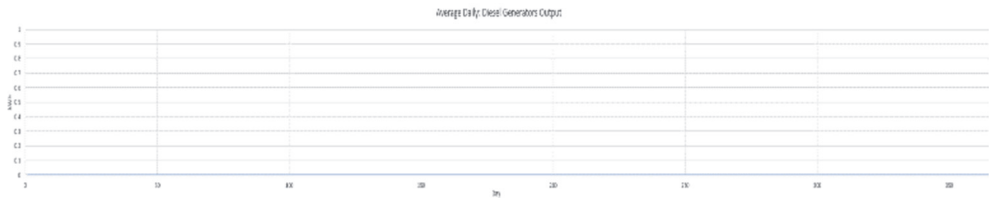


Figure 20: Daily averages of diesel generators contributions

The total electricity supplied to the system is represented in the following:

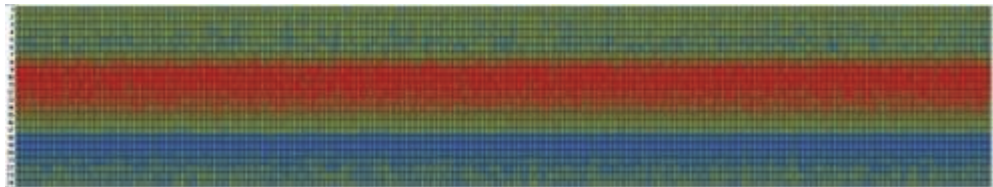


Figure 21: Hourly electricity supplied for an entire year

It is possible to see that there is an increase in energy supplied from hour 8 to hour 14 due to the effect the solar panels are having in the configuration proposed by the genetic algorithm. The daily average amount of electricity supplied is shown next:

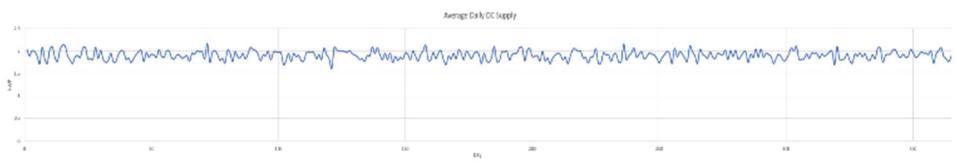


Figure 22: Daily averages of electricity supplied for an entire year

Next, we show the batteries charge state hour by hour for an entire year:

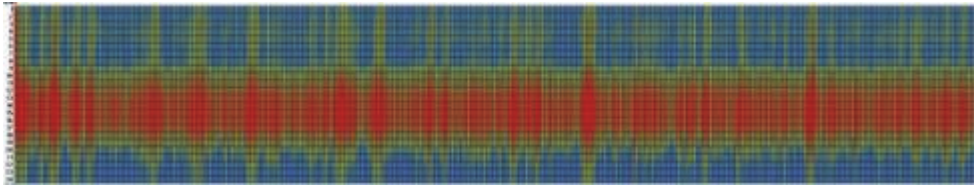


Figure 23: Batteries charge state hourly for an entire year

It is possible to see that the batteries are usually recharged during the day, mostly from hour 11 until hour 18, and then get discharged during the night to compensate the lack of electricity from the solar panels, as these do not produce electricity during the night. The average daily state of charge is shown in the next figure:



Figure 24: Daily average state of charge of the batteries for an entire year

And lastly, we show a graph depicting the hourly power grid purchases for an entire year as follows:

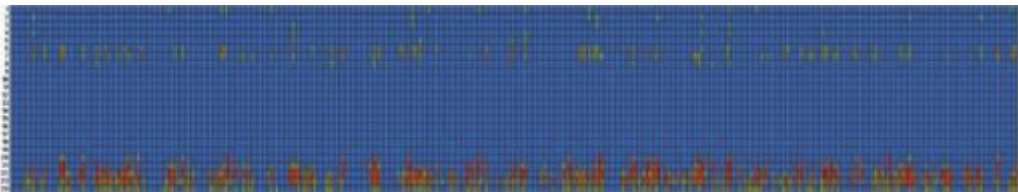


Figure 25: Hourly purchases of electricity from grid, for an entire year.

We can see from figure 25 that most of the purchases occur mostly during the night, to help the electric batteries in providing the necessary electricity to the microgrid whenever these get fully discharged. Then, we show the daily average amount of electricity purchased from the power grid in figure 26 next:

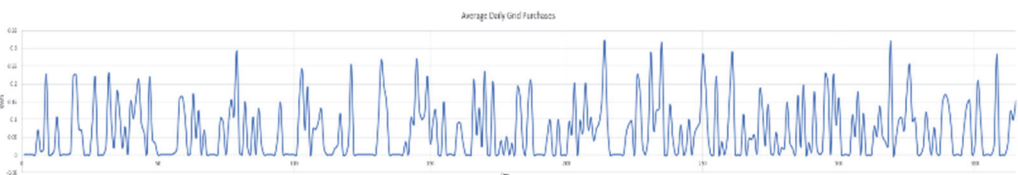


Figure 26: Daily averages of purchases from power grid.

It is notorious that some days there are plenty of purchases while in some other days there is no need to purchase any electricity from the power grid. The maximum amount purchased is 2.2 kW which is

equal to the maximum capacity. It is noted that the solution presented by the genetic algorithm incurs in some blackouts yielding a blackout annual worth of -4'000,000 which is the vast majority of the negative total annual worth of the microgrid configuration presented by the genetic algorithm.

5.2 Fireworks Algorithm Results

The fireworks algorithm yielded the following recommended solution:

- Recommended Number of Solar Panels: 0
- Recommended Number of Wind Turbines: 0
- Recommended Number of Diesel Generators: 1
- Recommended Number of Electric Batteries: 1
- Recommended Number of Converters: 1
- Recommended Connection to Power Grid: Yes
- Total Annual Worth = -29,996.2979 USD

The convergence is found after 126 generations, with the following distribution of improvement along the generations:

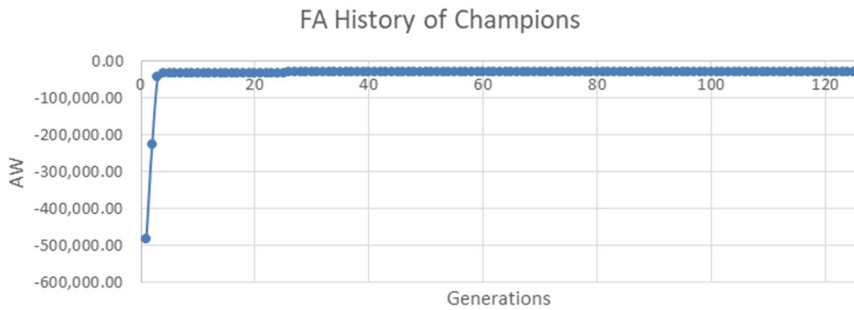


Figure 27: Evolution of alpha firework 'champion'

From the figure 27 above we notice great improvement on the first 5 generations after which the improvement was stable until convergence.

The yielded solution from the firework algorithm shows the following properties:

Regarding the annual electric demand distribution, a graphical representation is shown in the same fashion as the results shown before.

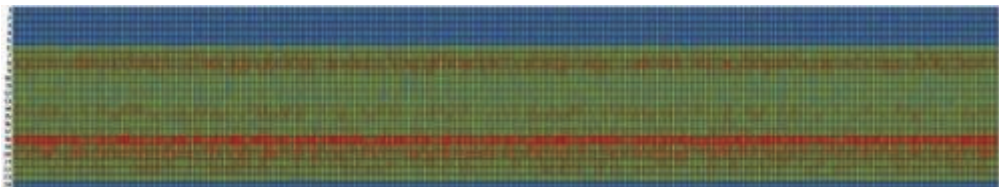


Figure 28: Hourly electric demand for an entire year

We notice a similar behaviour to the one presented previously in figure 13, where peak demand levels are mostly occurring by the 18 hour of the day, and low levels occur from hour 24 to hour 5 of the next day.

Following the same structure as before, we now show the average electric demand that occurred per day for an entire year:



Figure 29: Daily demand averages for an entire year

The daily averages are diverse and varied as expected. Next, the stripe graph below shows the solar panels output for each hour during an entire year:



Figure 30: Hourly solar panels electric contribution for an entire year

The hourly output shows red for all hours since there are no solar panels installed in the solution proposed by the fireworks algorithm, and consequently the daily averages of solar panels output for an entire year is also presenting zero values as shown next:

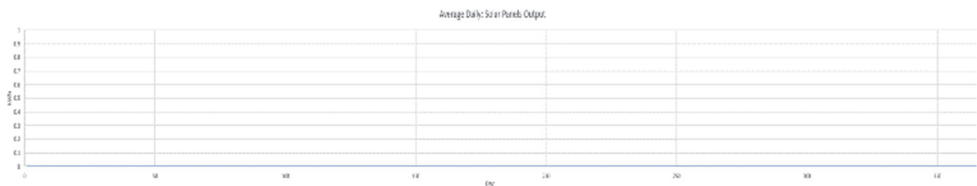


Figure 31: Daily solar panels contribution averages for an entire year

We see the amount of electricity provided by the wind turbines in the graph below is similarly zero, as there are no wind turbines installed in the solution proposed by the fireworks algorithm.



Figure 32: Hourly wind turbines contribution for an entire year

This means the daily average contributions of wind turbines for an entire year is also zero:

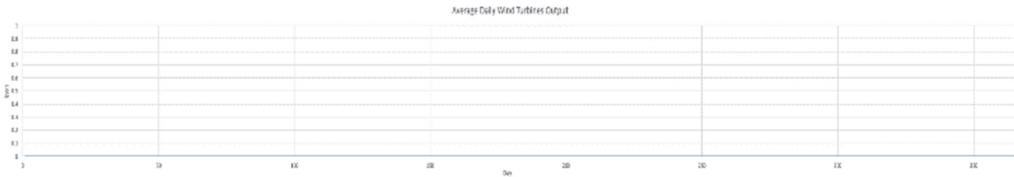


Figure 33: Daily wind turbines contribution averages for an entire year

Some values to note however, are the hourly contributions of diesel generators for an entire year, which are shown in figure 34 below. However, even with the red color showing in the stripe graph, the diesel generators are indeed producing 2.8 kWh of electricity, so the values are actually stable, just not in zero:



Figure 34: Hourly diesel generators contribution for an entire year

Next, the corresponding daily averages are 2.8 kWh as shown in figure 35:

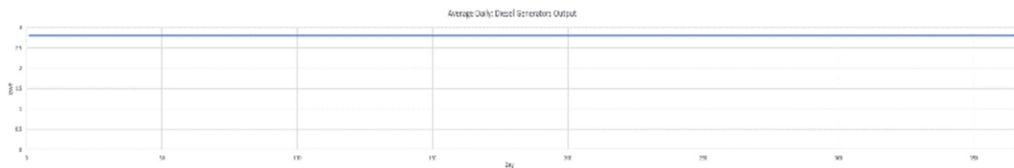


Figure 35: Daily averages of diesel generators contributions

The total electricity supplied to the system is represented in the following graph:



Figure 36: Hourly electricity supplied for an entire year

The electricity supplied is stable at a level of 2.8 kWh since only 1 diesel generator is contributing. This provokes that daily average amount of electricity supplied graph is also stable at 2.8 kWh as expected:

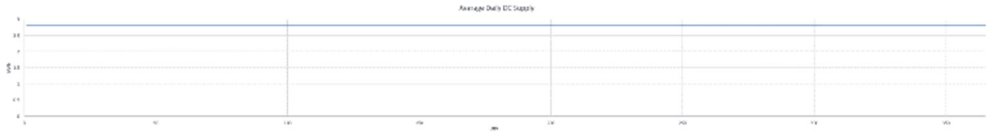


Figure 37: Daily averages of electricity supplied for an entire year

Next, we show the batteries charge state hour by hour for an entire year:

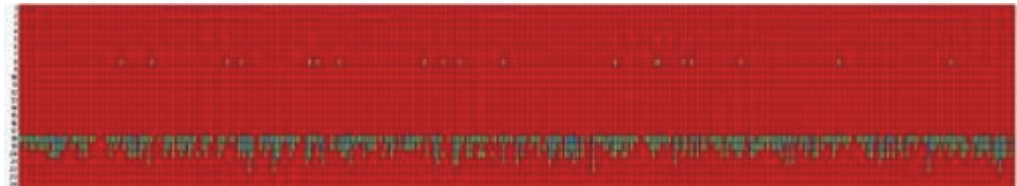


Figure 38: Batteries charge state hourly for an entire year

From figure 38 above we can see that the batteries are usually fully charged, and experiencing some discharges during the evening of most days, mostly corresponding to the peak electricity demand that occurs at hour 18, as shown on figure 28 shown before. Moreover, the average daily state of charge is shown in the next figure where we see that many days the state of charge is close to full charge, with exceptional days where it can significantly decrease:



Figure 39: Daily average state of charge of the batteries for an entire year

Moreover, the microgrid configuration found by the fireworks algorithm solution incurs in zero power grid purchases whatsoever with the exception for a single purchase at hour 20 of day 334 as shown next in figure 40:



Figure 40: Hourly purchases of electricity from grid, for an entire year.

And from the behaviour shown above, it is expected that the following graph presenting the daily averages of purchases from the power grid looks as follows with a single peak on day 334:

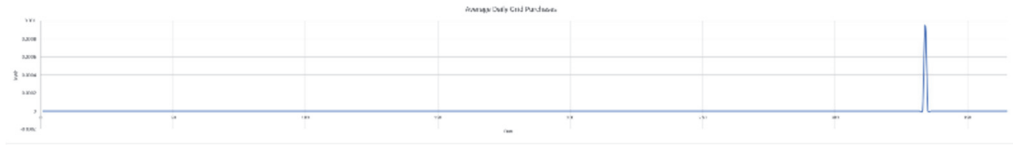


Figure 41: Daily averages of purchases from power grid.

The peak shown on figure 41 reveals that this configuration presented by the fireworks algorithm is using the power grid connection as an emergency failsafe to provide electricity whenever it is not available in the electric battery, but not as a primary source of electricity.

5.3 Hybrid Genetic-Fireworks Algorithm Results

The hybrid genetic-fireworks algorithm yielded the following recommended solution:

- Recommended Number of Solar Panels: 0
- Recommended Number of Wind Turbines: 0
- Recommended Number of Diesel Generators: 1
- Recommended Number of Electric Batteries: 1
- Recommended Number of Converters: 1
- Recommended Connection to Power Grid: Yes
- Total Annual Worth = -29,996.2874 USD

The convergence is found after 82 generations, with the following distribution of improvement along the generations:

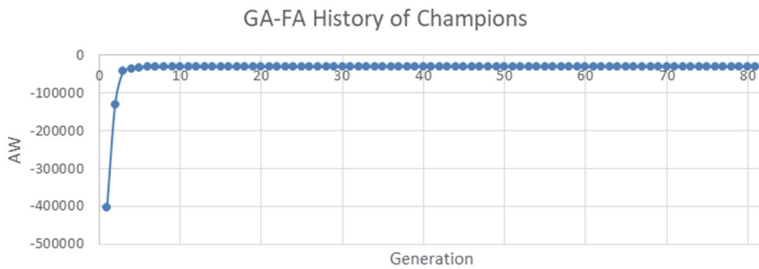


Figure 42: Evolution of alpha firework 'champion'

From the figure 42 above we notice great improvement on the first 7 generations after which the improvement was gradually stabilizing until convergence. The yielded solution from the firework algorithm shows the following properties:

Regarding the annual electric demand distribution, the pattern is the following.

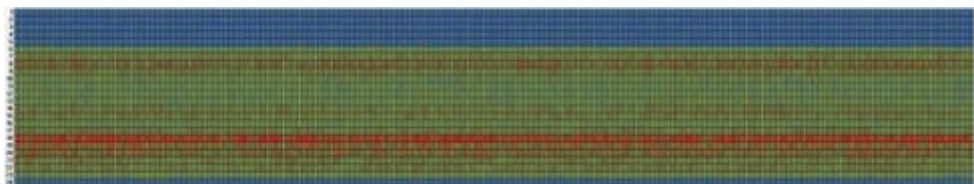


Figure 43: Hourly electric demand for an entire year

We notice a similar behaviour to the others presented previously in figures 13 and 28 for the solutions found by genetic algorithm and fireworks algorithm. This is expected as the Monte Carlo simulation randomly produces weather conditions for each solution that are different from each other but still statistically similar.

The average daily electric demand day for an entire year is the following:

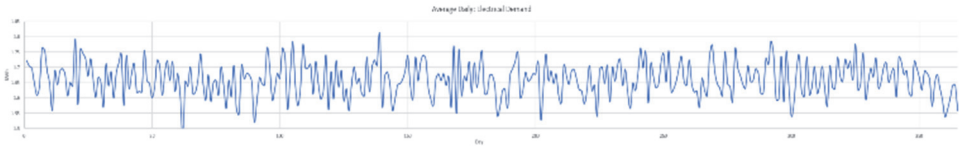


Figure 44: Daily demand averages for an entire year

The daily averages continue to be varied. Next, the hourly solar panels output for an entire year is shown:



Figure 45: Hourly solar panels electric contribution for an entire year

The hourly output is also red for the solution of the hybrid algorithm since there are no solar panels installed, and therefore the daily averages of electricity provided by solar panels is also presenting zero:

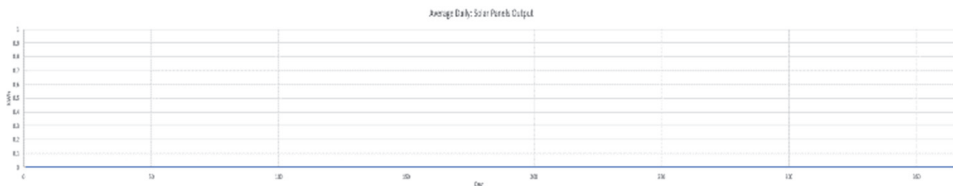


Figure 46: Daily solar panels contribution averages for an entire year

We see the amount of electricity provided by the wind turbines in the graph below is another zero, since no wind turbines whatsoever are installed in the solution proposed by the hybrid algorithm.



Figure 47: Hourly wind turbines contribution for an entire year

This means the daily average contributions of wind turbines for an entire year is also zero:

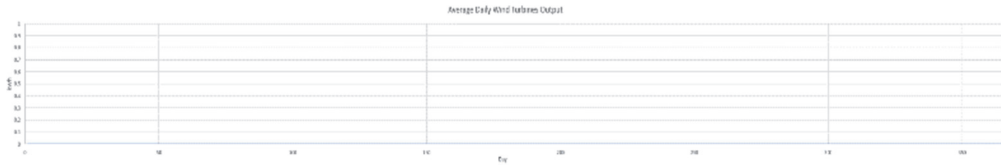


Figure 48: Daily wind turbines contribution averages for an entire year

It is noteworthy that the hourly contributions of diesel generators shown below in figure 49 is stable at 2.8 kWh of electricity:



Figure 49: Hourly diesel generators contribution for an entire year

Next, as expected the corresponding daily averages are 2.8 kWh as shown in figure 50:

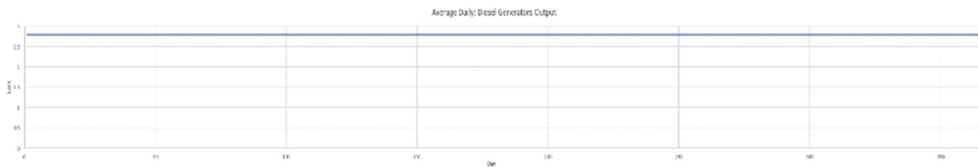


Figure 50: Daily averages of diesel generators contributions

The total electricity supplied to the system is represented in the following graph:



Figure 51: Hourly electricity supplied for an entire year

The electricity supplied is 2.8 kWh every hour. This flat behaviour causes that daily average amount of electricity supplied graph is also 2.8 kWh:

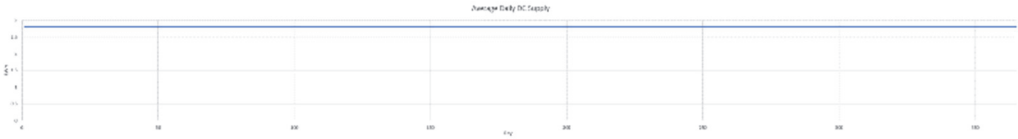


Figure 52: Daily averages of electricity supplied for an entire year

Next, we show the batteries' state of charge by the hour for an entire year:



Figure 53: Batteries charge state hourly for an entire year

The behaviour is virtually the same as the one exhibited during the to the solution found by the fireworks algorithm: mostly charged and some discharges during the peak demand hour. Moreover, the daily average state of charge of the batteries is shown:

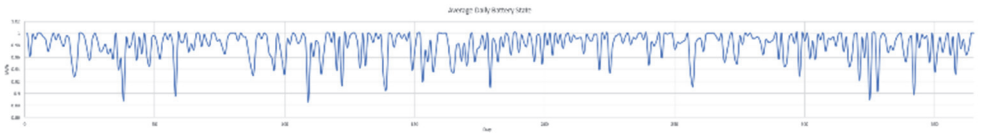


Figure 54: Daily average state of charge of the batteries for an entire year

Now, in regards of power grid purchases, the solution presented by the hybrid algorithm doesn't incur in any power grid purchased as shown next in figure 55.



Figure 55: Hourly purchases of electricity from grid, for an entire year.

And from the behaviour shown above, it is expected that the following graph is also full of zeros values:

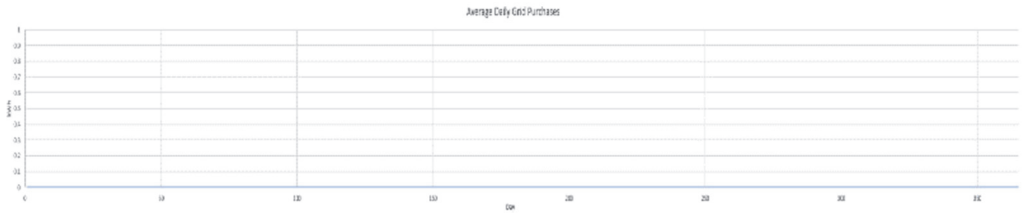


Figure 56: Daily averages of purchases from power grid.

The solutions found by the fireworks algorithm and the hybrid genetic-fire algorithm are the same, and these similarities and differences are discussed next.

6. Discussion

For a better discussion of the results obtained by the 3 algorithms, we show the following table:

Table 4: Performance Comparison

Item	Genetic Algorithm	Fireworks Algorithm	Hybrid Algorithm
Recommended Solar Panels	39	0	0
Recommended Wind Turbines	1	0	0
Recommended Diesel Generators	0	1	1
Recommended Electric Batteries	16	1	1
Recommended Converters	1	1	1
Recommended Power Grid	Yes	Yes	Yes
AW Solar Panels	-15,933.52	0.00	0.00
AW Wind Turbines	-45,240.31	0.00	0.00
AW Diesel Generator	0.00	-853.65	-853.65
AW Fuel	0.00	-29,108.60	-29,108.60
AW Batteries	-314.25	-19.64	-19.64
AW Converter	-14.39	-14.39	-14.39
AW PowerGrid	0.00	0.00	0.00
AW Electricity Purchased	-259.45	-0.01	0.00
AW Blackout	-4,000,000.00	0.00	0.00
AW Total	-4,061,761.92	-29,996.30	-29,996.29
COE	279.75	2.06	2.06
Total Generations to Converge	217.	126	82
Time taken (seconds)	3,977.72	11,042.98	8,527.05
Bytes allocated (memory used)	3.74659E+12	7.91141E+12	6.43988E+12

From the table 4 above we see that the fireworks algorithm as well as the hybrid genetic-fireworks algorithm arrive to the same microgrid configuration. Moreover, they both yield an annual worth of -29,996, and this makes sense since the same configuration is evaluated by the Monte Carlo simulation 2 different times as these are coming from different optimization algorithms. Moreover, there is outperformance evidence by the hybrid genetic-fireworks algorithm over the fireworks algorithm in regards of requiring less generations to converge: 82 versus 126. We also notice a small difference between the evaluation of the fireworks algorithm and the hybrid genetic-fireworks algorithm even when the configuration is the same, and this small difference is explained since the Monte Carlo simulation is using probabilistic approach to model the behaviour of the microgrid, hence the electric demands and weather conditions are slightly different from each other, as is

expected.

The cost of energy (COE) shown below the total annual worth (AW Total) represents the cost of consuming 1 kWh of electricity when using the microgrid configurations that are recommended by the optimization algorithms correspondingly.

It seems the genetic algorithm is performing noticeably worse than the other 2 algorithms with the most negative annual worth, and taking the most generations to converge.

7. Conclusion

We highlight the following findings:

Finding 1: The hybrid genetic-fireworks algorithm is outperforming the other 2 algorithms, and as such we recommend it for further exploitation in finding solutions to the renewable energy integration problem.

Finding 2: It appears that even with inflated prices for electricity, inflated prices for fuel, and high interest rates, the preference was still biased towards purchasing electricity from the power grid and the use of diesel generators.

Finding 3: It was noted that the Cost of Energy (COE) in the configurations found by the stochastic algorithms is still higher than the cost of purchasing electricity from the power grid, and as such we suspect that until this cost decreases to levels that are lower than the purchasing price from the power grid, there is a high likelihood that convergence will occur in favor of utilizing the existing power grids available.

Finding 4: It appears that a harsh economic environment is not sufficient argument on its own to prefer renewable energy over fossil fuel electricity, at least on a micro-grid level, since the type of solutions found by the optimization algorithms where zero renewable energy fraction.

As a final conclusion, we theorize that the size in capacity of the renewable energy components may be an important factor in guiding the final decision proposed by the stochastic algorithms, into configurations that are using more renewable energy, if considering purely economic arguments. And since microgrids are usually private properties of limited size, it makes sense for these properties to require relatively small sizes of components to satisfy their demand, hence making it a bad investment for small property owners (houses of 5 people or less) as shown in this paper.

References

- EIA (2023). China Country Analysis Brief. U.S. Department of Energy. U.S. Energy Information Administration. Washington DC 20585. www.eia.gov, https://www.eia.gov/international/content/analysis/countries_long/China/pdf/china-2023.pdf
- Faizan A. (2023). Electrical Academia. <https://electricalacademia.com/renewable-energy/wind-turbine-power-curve/>
- Hubbert, M. K. (1956). Nuclear energy and the fossil fuels (Vol. 95). Houston, TX: Shell Development Company, Exploration and Production Research Division.
- IEA (2019). Top ten electricity consuming countries, 2019. International Energy Agency, Paris <https://www.iea.org/data-and-statistics/charts/top-ten-electricity-consuming-countries-2019>, IEA. Licence: CC BY 4.0
- IEA (2021). Electricity Information: Overview. International Energy Association, Paris <https://www.iea.org/report-s/electricity-information-overview>, License: CC BY 4.0
- IEA, Electricity generation by source, OECD, 2000-2020. International Energy Association, Paris <https://www.iea.org/data-and-statistics/charts/electricity-generation-by-source-oecd-2000-2020>, IEA. Licence: CC BY 4.0
- Jadoun, V. K., Pandey, V. C., Gupta, N., Niazi, K. R., & Swarnkar, A. (2018). Integration of renewable energy sources in dynamic economic load dispatch problem using an improved fireworks algorithm. IET renewable power generation, 12(9), 1004-1011.

- Epa, K., Cpalka, K. (2016). On the Application of a Hybrid Genetic-Firework Algorithm for Controllers Structure and Parameters Selection. In: Borzemski, L., Grzech, A., Świątek, J., Wilimowska, Z. (eds) Information Systems Architecture and Technology: Proceedings of 36th International Conference on Information Systems Architecture and Technology – ISAT 2015 – Part I. Advances in Intelligent Systems and Computing, vol 429. Springer, Cham. https://doi.org/10.1007/978-3-319-28555-9_10
- Lopez N., Hoti A. and Takeaki T. (2023). Renewable Energy Integration on a High Inflation Economic Scenario by means of Firework Algorithm, Genetic Algorithm and Monte Carlos Simulation. *Academic Journal of Interdisciplinary Studies*. 12(6), pp. 319-334.
- M. J. Mayer, A. Szilágyi, G. Gróf. (2020). Environmental and economic multi-objective optimization of a household level hybrid renewable energy system by genetic algorithm. *Applied Energy*, Volume 269, ISSN 0306-2619, <https://doi.org/10.1016/j.apenergy.2020.115058>.
- M.S. Ismail, M. Moghavvemi, T.M.I. Mahlia. (2014). Genetic algorithm based optimization on modeling and design of hybrid renewable energy systems. *Energy Conversion and Management*, Volume 85, Pages 120-130. ISSN 0196-8904. <https://doi.org/10.1016/j.enconman.2014.05.064>.
- NASA (2018). Prediction of Worldwide Energy Resources (POWER) [database]. <https://power.larc.nasa.gov/>
- OECD (2021). OECD Reviews of Innovation Policy: Kuwait 2021. Organisation for Economic Co-operation and Development (OECD). December 10, 2021. <https://www.oecd.org/countries/kuwait/oecd-reviews-of-innovation-policy-kuwait-2021-49ed2679-en.htm>
- OECD (2022). Global Forum on Transparency and Exchange of Information for Tax Purposes: Kuwait 2022 (Second Round, Phase 1). Organisation for Economic Co-operation and Development (OECD). November 9, 2022. <https://www.oecd.org/countries/kuwait/global-forum-on-transparency-and-exchange-of-information-for-tax-purposes-kuwait-2022-second-round-phase-1-45cceed-en.htm>
- OECD (2023). Kuwait joins the Inclusive Framework on BEPS and participates in the agreement to address the tax challenges arising from the digitalisation of the economy. Centre for Tax Policy and Administration Communications Office (CTPA). Organisation for Economic Co-operation and Development (OECD). 15-November-2023. <https://www.oecd.org/countries/kuwait/kuwait-joins-the-inclusive-framework-on-beps-and-participates-in-the-agreement-to-address-the-tax-challenges-arising-from-the-digitalisation-of-the-economy.htm>
- S. Shafiee, and E. Topal. (2009). When will fossil fuel reserves be diminished?. *Energy Policy*, Volume 37, Issue 1, Pages 181-189. <https://doi.org/10.1016/j.enpol.2008.08.016>.
- Sobol, Ilya M. (2017). A Primer for the Monte Carlo Method. CRC Press. Boca Raton 30 September 2017. ISBN 9781315136448. <https://doi.org/10.1201/9781315136448>
- Swart, J. (2016). Testing a price breakout strategy using Donchian Channels. (Thesis). University of Cape Town, Faculty of Commerce, Department of Finance and Tax. Retrieved from <http://hdl.handle.net/11427/21754>
- UN (2022). World Population Prospects 2022. Online Edition. United Nations, Department of Economic and Social Affairs, Population Division. File GEN/01/REV1: Demographic indicators by region, subregion and country, annually for 1950-2100. Medium fertility variant, 2022-2100. POP/DB/WPP/Rev.2022/GEN/F01/Rev.1 <http://creativecommons.org/licenses/by/3.0/igo/>
- W. G. Sullivan, E. M. Wicks, C. P. Koelling. (2014). *Engineering Economy* 16th Edition. Pearson Education. ISBN 978-0-13-255490-9
- Wang, Z., Zhu, Q., Huang, M., & Yang, B. (2017). Optimization of economic/environmental operation management for microgrids by using hybrid fireworks algorithm. *International Transactions on Electrical Energy Systems*, 27(12), e2429.